MOLECULAR AND CELLULAR BIOLOGY, Jan. 2005, p. 854–864 Vol. 25, No. 2
0270-7306/05/$08.00+0 doi:10.1128/MCB.25.2.854–864.2005

Extracellular Signal-Regulated Kinases Phosphorylate Mitogen-Activated Protein Kinase Phosphatase 3/DUSP6 at Serines 159 and 197, Two Sites Critical for Its Proteasomal Degradation

Sandrine Marchetti,†‡ Clotilde Gimond,†* Jean-Claude Chambard, Thomas Touboul, Danièle Roux, Jacques Pouysségur, and Gilles Pagès

Institute of Signaling, Developmental Biology and Cancer Research, CNRS UMR 6543, Centre Antoine Lacassagne, Nice, France

Received 30 April 2004/Returned for modification 3 June 2004/Accepted 28 October 2004

Mitogen-activated protein (MAP) kinase phosphatases (MKPs) are dual-specificity phosphatases that dephosphorylate phosphothreonine and phosphotyrosine residues within MAP kinases. Here, we describe a novel posttranslational mechanism for regulating MKP-3/Pyst1/DUSP6, a member of the MKP family that is highly specific for extracellular signal-regulated kinase 1 and 2 (ERK1/2) inactivation. Using a fibroblast model in which the expression of either MKP-3 or a more stable MKP-3–green fluorescent protein (GFP) chimera was induced by tetracycline, we found that serum induces the phosphorylation of MKP-3 and its subsequent degradation by the proteasome in a MEK1 and MEK2 (MEK1/2)-ERK1/2-dependent manner. In vitro phosphorylation assays using glutathione *S*-transferase (GST)–MKP-3 fusion proteins indicated that ERK2 could phosphorylate MKP-3 on serines 159 and 197. Tetracycline-inducible cell clones expressing either single or double serine mutants of MKP-3 or MKP-3–GFP confirmed that these two sites are targeted by the MEK1/2-ERK1/2 module in vivo. Double serine mutants of MKP-3 or MKP-3–GFP were more efficiently protected from degradation than single mutants or wild-type MKP-3, indicating that phosphorylation of either serine by ERK1/2 enhances proteasomal degradation of MKP-3. Hence, double mutation caused a threefold increase in the half-life of MKP-3. Finally, we show that the phosphorylation of MKP-3 has no effect on its catalytic activity. Thus, ERK1/2 exert a positive feedback loop on their own activity by promoting the degradation of MKP-3, one of their major inactivators in the cytosol, a situation opposite to that described for the nuclear phosphatase MKP-1.

Extracellular signal-regulated kinases (ERKs) are central to numerous biological responses, including cell growth, differentiation, and survival. ERK1 and ERK2 (ERK1/2; also referred to as p44/p42 mitogen-activated protein [MAP] kinases) are activated through the stimulation of tyrosine kinase receptors, G protein-coupled receptors, and integrins (30). Receptor ligation leads to the activation of the small G protein ras, followed by the recruitment of the raf kinase to the membrane and by subsequent activation of downstream kinases, MEK1 and MEK2 (MEK1/2) and ERK1/2. Once activated by phosphorylation on both Thr and Tyr residues, ERK1/2 phosphorylate in turn numerous substrates in the cytosol, the nucleus, and the plasma membrane (30).

The activity of ERK1 and ERK2 is tightly regulated in a spatiotemporal manner that is determinantal for their biological action (31). Inactivation of ERKs following exposure to a mitogenic signal occurs in two steps. Different phosphatases with a Ser/Thr (PP2A) or a Tyr (PTP-SL, STEP, and He-PTP/LC-PTP) specificity are involved in the initial step, corresponding to a rapid inactivation of ERK1 and ERK2 (1, 31). These phosphatases are constitutively expressed in the cell. In contrast, the delayed phase of ERK inactivation is dependent on new gene expression and protein synthesis, implying more specific phosphatases with a dual specificity for Ser/Thr and Tyr and referred to as MAP kinase phosphatases (MKPs) (6, 18, 38).

The MKP family, which belongs to the dual-specificity phosphatase (DUSP) family, is defined by a common structure, comprising a C-terminal catalytic domain sharing sequence homology with the DUSP VH1 and an N-terminal noncatalytic domain containing two regions homologous to sequences found in the phosphatase cdc25. Ten MKPs, which exhibit differential specificities towards their MAP kinase (MAPK) substrates as well as distinct subcellular localizations and modes of regulation, have been described so far. While MKP-1 and MKP-2, also called DUSP1 and DUSP4, are strictly nuclear and dephosphorylate both ERKs and the stress-activated protein kinases p38 MAPK and c-Jun N-terminal kinase (JNK), MKP-3, also called Pyst-1 or DUSP6, is cytoplasmic and specific to ERKs (6, 18, 28, 37). Apart from ERK1 and ERK2, MKP-3 can also dephosphorylate ERK5, another MAPK family member downstream of MEK5 activated by diverse stimuli, including growth factors (14, 16).

The genes encoding MKP-1 and MKP-2 are early genes, rapidly induced by both stress and growth factors with direct involvement of ERKs (3, 7, 15). The regulation of MKP-3 expression is, however, still a matter of controversy. Depending on the study, and possibly on the different cell lines for which

* Corresponding author. Mailing address: Institute of Signaling, Developmental Biology and Cancer Research, CNRS UMR 6543, Centre Antoine Lacassagne, 33 Ave. de Valombrose, 06189 Nice, France. Phone: (33) 492 03 12 31. Fax: (33) 492 03 12 35. E-mail: gimond@unice.fr.

† S.M. and C.G. contributed equally to this work.

‡ Present address: INSERM U526, Physiopathologie de la Survie et de la Mort Cellulaires et Infections Virales, 06107 Nice, France.

it was analyzed, MKP-3 expression appears to be either constitutive in some cell types (13) or induced by some growth factors, including nerve growth factor and basic fibroblast growth factor (5, 32).

The regulation of MKPs by ERKs also takes place at a more direct, posttranslational level. Hence, both MKP-1 and MKP-3 are activated through conformational changes upon binding of their N-terminal domain to ERKs. This phenomenon is independent of ERK activity. In MKP-3, the N-terminal domain does not allow firm interaction with p38 MAPK and JNK, thereby ensuring the specificity of the dephosphorylation event towards ERK1 and ERK2 (reviewed in references 6 and 18).

Phosphorylation of MKP-1 and MKP-2 by ERKs provides an additional level of regulation of this phosphatase by reducing its rate of degradation by the proteasome (3, 35). However, nothing is known about the regulation of MKP-3 stability. Because, in contrast to MKP-1 and MKP-2, MKP-3 displays a high specificity towards ERK1/2 and an exclusive cytosolic localization, the regulation of its stability may follow a distinct scheme.

The purpose of the present work was to investigate whether MKP-3 undergoes posttranslational modification that could affect its stability. We have identified two serine residues in the N-terminal domain of MKP-3 which are modified by ERKs in vitro and phosphorylated following activation of the MEK1/2-ERK1/2 pathway in cells. In addition, our results indicate that, in contrast to the results obtained with the nuclear MAPK phosphatases (MKP-1 and MKP-2), phosphorylation of MKP-3 enhanced its degradation by the proteasome.

MATERIALS AND METHODS

Materials. Restriction and DNA-modifying enzymes and calf intestine phosphatase (CIP) were obtained from New England Biolabs (Beverly, Mass.) or from Eurogentec (Seraing, Belgium). Synthetic oligonucleotides were from Cybergene (Evry, France) and Eurogentec. Tetracycline, 4-hydroxytamoxifen (4-OHT), and *N*-acetyl-Leu-Leu-norleucinal (LLnL) were obtained from Sigma (St. Louis, Mo.). U0126 and SB202190 were from Calbiochem (Meudon, France). PD184352 was a kind gift of Philip Cohen (University of Dundee, Dundee, United Kingdom).

Antibodies. Specific antisera directed against MKP-3/Pyst1 and ERK1/2 have been previously characterized (4, 21). The monoclonal antibody directed against dual-phosphorylated ERK1/2 was purchased from Sigma. For immunoprecipitation experiments, polyclonal antibodies directed against the transcription factor Sp3 and against MKP-3 were purchased from Santa Cruz Biotechnology (Santa Cruz, Calif.). The antibody directed against ERK5 was kindly provided by Philip Cohen (University of Dundee).

Horseradish peroxidase (HRP)-conjugated anti-mouse and anti-rabbit antibodies were purchased from Promega (Charbonnières, France). The HRP-conjugated anti-sheep antibody was purchased from DakoCytomation (Copenhagen, Denmark).

Plasmid construction and site-directed mutagenesis. MKP-3 cDNA cloned into the pSG5 vector (Stratagene, La Jolla, Calif.) was kindly provided by Stephen Keyse (4), and the MKP-3–green fluorescent protein (GFP) fusion cDNA vector was previously described (24). Both cDNAs were subsequently subcloned into pcDNA4/TO/myc-His (Invitrogen, Leek, The Netherlands).

The pcDNA4/TO-MKP-3-229 truncated mutant was obtained by subcloning the EcoRI fragment of MKP-3 into the same site of the pcDNA4/TO/myc-His vector. Serine mutations in both the pcDNA4/TO-MKP-3 and MKP-3–GFP constructs were generated by using the Stratagene site-directed mutagenesis kit and the following couples of oligonucleotides: 5′-GCTCGTGTAGCAGCAGC GCGCCGCCGTTGCCAGTGC66-3′ and 5′-GCACTGGCAACGGCGGCGC GCTGCTGCTACACGAGC-3′ (Ser159 to Ala mutation) and 5′-GCAACAGA CTCGGATGGTGCTCCGCTGTCCAACAGCC-3′ and 5′-GGCTGTTGGAC AGCGGAGCACCATCCGAGTCTGTTGC-3′ (Ser197 to Ala mutation).

pGEX-6P1 plasmids coding for glutathione *S*-transferase (GST)–MKP-3 fusion proteins were constructed as follows: full-length MKP-3 was amplified by PCR from the pSG5-MKP-3 vector by using the oligonucleotide 5′-GCAGGA TCCATAGATACGCTCAGACCCGTG-3′, in which the START codon of MKP-3 was replaced by a BamHI restriction site, and the oligonucleotide 5′-G CACTCGAGCGTAGATTGCAGAGAGTCCAC-3′, containing an XhoI site, and subsequently cloned into the same sites of the pGEX-6P1 vector (Amersham Biosciences, Saclay, France). The ΔC346 truncation mutant of MKP-3 was also constructed by PCR by replacing the above described 3′ oligonucleotide with 5′-GCACTCGAGCCTCTCGAAGTCCAGCAGCTG-3′ and using the same restriction sites. The pGEX-6P1-MKP-3-C/S full-length and ΔC346 mutants were also constructed by PCR with the same oligonucleotides but by using pSG5-MKP-3-C/S as a template (13).

For the GST–MKP-3-ΔC229 mutant, the BamHI-EcoRI fragment of pGEX-6P1-MKP-3 (corresponding to the N-terminal domain of MKP-3) was digested and subcloned into pGEX-6P1. The plasmid coding for the ΔN-MKP-3 truncation mutant was constructed by subcloning the EcoRI-XhoI fragment of MKP-3 into the same sites of pGEX-6P1.

The cDNA of rat ERK1 was cloned in the EcoRI sites of pGEX-2T for production of GST-ERK1.

Cell culture and transfection. Clone S19R443, derived from the CCL39 hamster fibroblast cell line and expressing both the ΔRaf1:estrogen receptor (ER) chimera and the tetracycline repressor, has been previously described (25). These cells were used for further transfection with either pcDNA4/TO-MKP-3 or pcDNA4/TO-MKP-3–GFP, as described by Marchetti et al. (24), or with pcDNA4/TO plasmids encoding MKP-3 and MKP-3–GFP mutants. Zeocine-resistant clones were screened by immunofluorescence and Western blotting after tetracycline induction (1 μg/ml).

Metal affinity precipitation of ubiquitinated proteins. Precipitation of ubiquitinated proteins was done essentially as described previously (9). Briefly, HeLa cells were cotransfected with the pSG5-MKP-3 plasmid and with pRBG4-six-HisUb (30 μg/5 × 10^6 cells). Thirty hours after transfection, cells were lysed in ULB (8 M urea, 20 mM Tris-HCl [pH 7.5], 200 mM NaCl, 10 mM imidazole, and 0.1% Triton X-100). Next, lysates were purified for histidine-tagged ubiquitin on 30 μl of cobalt-chelated resin (Clontech) that had been previously incubated in 5% bovine serum albumin (radioimmunoassay grade; Sigma). After lysate incubation, the beads were washed four times in ULB and once in phosphate-buffered saline (PBS) and resuspended in 1 volume of Laemmli buffer. Proteins were resolved by sodium dodecyl sulfate–7.5% polyacrylamide gel electrophoresis (SDS–7.5% PAGE), and polyubiquitylated MKP-3 was visualized by immunoblotting.

Western blotting. Cells from MKP-3 or MKP-3–GFP-inducible clones were seeded in 12-well plates at a density of 10^5 cells per well and grown for 48 h in Dulbecco's modified Eagle medium containing 7.5% serum. Cells were next serum starved for 20 h in the absence or presence of 1 μg of tetracycline/ml to induce transgene expression. Cells were then stimulated for various times with either 20% fetal calf serum or 1 μM 4-OHT (for the activation of the ΔRaf1:ER chimera). In some experiments, cells were preincubated either for 4 h with LLnL (50 μM) or for 45 min with cycloheximide (10 μg/ml) to block proteasomal activity or protein neosynthesis, respectively. After two washes with ice-cold PBS, cells were immediately lysed in Laemmli sample buffer. Proteins were quantified with a bicinchoninic acid (BCA) kit (Sigma), resolved on SDS–10% PAGE gels (made with acrylamide-bisacrylamide [37.5:1]; Sigma), and transferred onto polyvinylidene difluoride membranes (Immobilon-P; Polylabo, Strasbourg, France). Membranes were incubated with the appropriate specific primary antibody followed by the corresponding HRP-conjugated secondary antibody, and proteins were detected by enhanced chemiluminescence (Amersham Biosciences). When indicated, protein levels were quantified with the Gene Gnome (Syngene Bio Imaging).

For experiments with CIP, cells were first lysed on ice in 1% Triton X-100 lysis buffer (50 mM Tris [pH 7.5], 100 mM NaCl, 0.5 mM EDTA). CIP (20 U/ml) was then added to the lysates, which were incubated for 30 min at 30°C. The reaction was stopped by adding Laemmli sample buffer.

Metabolic labeling with [^{33}P]orthophosphate and immunoprecipitation of endogenous MKP-3. S19 parental cells, expressing the ΔRaf1:ER chimera, were serum starved for 16 h in a phosphate-free medium supplemented with 20 μCi of [^{33}P]orthophosphate/ml. Cells were then stimulated in the presence of LLnL (50 μM) for 4 h with tamoxifen and lysed in 1% Triton X-100 lysis buffer (1% Triton X-100, 50 mM Tris [pH 7.5], 100 mM NaCl, 5 mM EDTA, 50 mM sodium fluoride, 40 mM β-glycerophosphate, 200 μM sodium orthovanadate, 5 μg of aprotinin/ml, 0.7 μg of pepstatin/ml, 0.5 μg of leupeptin/ml, and 0.1 mM phenylmethylsulfonyl fluoride). Clarified lysates were then submitted to immunoprecipitation with two different antibodies preabsorbed onto protein A-Sepharose (Pharmacia). First, protein extracts were incubated with an irrelevant antibody directed against the transcription factor Sp3 as a negative control.

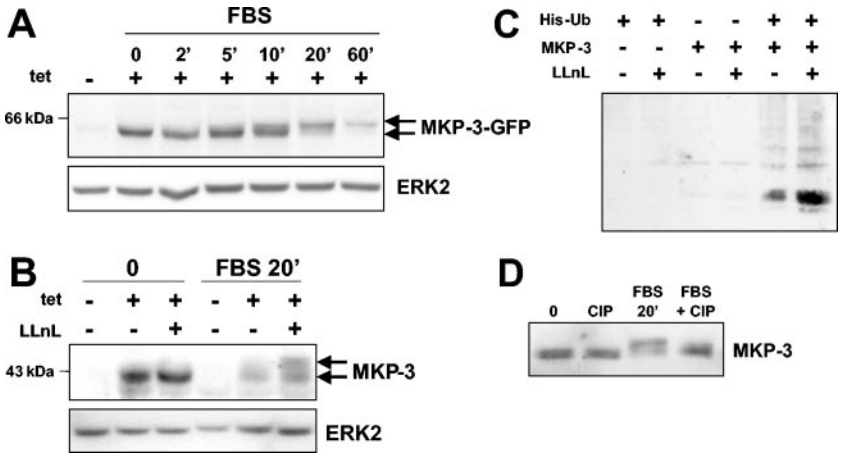

FIG. 1. Serum induces the phosphorylation of MKP-3. (A) Serum induces a shift in the electrophoretic mobility of MKP-3–GFP. Cells expressing MKP-3–GFP under the control of tetracycline were starved for 20 h and stimulated with 20% FBS for the indicated times (in minutes). Levels of MKP-3–GFP were analyzed by Western blotting with a polyclonal anti-MKP-3 antibody. Levels of ERK2 were taken as a loading control. (B) Serum induces a shift of native MKP-3 (uncoupled to GFP). Cells expressing a native form of MKP-3 under the control of tetracycline were starved for 20 h and stimulated or not with 20% FBS for 20 min. Levels of MKP-3 were analyzed by Western blotting, and ERK2 levels were taken as a loading control. When indicated, cells were pretreated with 10 μg of LLnL/ml for 20 h. Note that the higher-molecular-weight form of MKP-3 is stabilized by LLnL. (C) MKP-3 is ubiquitinated in vivo. HeLa cells were cotransfected with plasmids encoding MKP-3 and His-tagged ubiquitin. Ubiquitinated proteins were precipitated as described in Materials and Methods, and polyubiquitinated MKP-3 was revealed by Western blotting. (D) Treatment of cell lysates with CIP reverses the shift of MKP-3. Cells expressing MKP-3 under the control of tetracycline were starved, stimulated with FBS for 20 min, and then lysed in 1% Triton X-100 lysis buffer as described in Materials and Methods. Lysates were then incubated or not with CIP for 30 min at 30°C. The mobility of MKP-3 was analyzed by Western blotting.

Then, precleared supernatants were incubated with a specific antibody directed against MKP-3 (Santa Cruz Biotechnology). After 1 h at 4°C, immunocomplexes were washed three times with lysis buffer, boiled in Laemmli loading buffer, and separated by SDS-PAGE (10% acrylamide). Radiolabeled proteins were analyzed by autoradiography.

In vitro ERK assay. GST fusion proteins were produced from BL21 bacteria transformed with either pGEX-6P1 vector, as previously described (34). The assay was performed in kinase buffer (20 mM Tris, pH 7.5, 10 mM *p*-nitrophenylphosphate [*p*-NPP], 10 mM $MgCl_2$, 2 mM dithiothreitol) containing 30 U of recombinant active p42 MAPK/Erk2 (New England Biolabs), GST proteins, and 5 μCi of [γ-^{32}P]ATP (Amersham Biosciences) for 30 min at 30°C. The reaction was stopped by addition of Laemmli sample buffer and resolved on SDS-PAGE.

In vitro phosphatase assay. Phosphatase activity was measured as previously described (7). Briefly, samples were measured in 96-well plates in 200 μl of 50 mM imidazole (pH 7.5) containing 5 mM dithiothreitol, 20 μM *p*-NPP, and various concentrations of GST–MKP-3 and GST-ERK1. Reaction rates were measured at 405 nm in a microplate reader (Labsystems).

Immunofluorescence. Cells were grown on coverslips, starved overnight, and treated or not treated with tetracycline to induce MKP-3–GFP expression. Cells were then fixed in 3.3% paraformaldehyde, permeabilized in PBS containing 0.5% Triton X-100, blocked in 20% fetal bovine serum (FBS), and stained with the anti-MKP-3 antibody. Cells were next labeled with an anti-rabbit secondary antibody coupled to biotin, followed by staining with Alexa594-coupled streptavidin (Molecular Probes, Eugene, Oreg.). Cells were observed by confocal microscopy (Leica).

RESULTS

Serum induces phosphorylation of MKP-3 and degradation of MKP-3 by the proteasome machinery. We recently described a fibroblast cell system, derived from the Chinese hamster CCL39 cell line, in which the expression of either the MKP-3 phosphatase or a chimeric MKP-3–GFP can be induced by tetracycline. It was shown that the fusion of GFP strongly increased the stability of MKP-3, thereby allowing efficient blockade of the ERK signaling pathway and cell growth, in vitro as well as in vivo (24). Using the same cellular model, we now report that serum stimulation of previously starved cells causes a change in the electrophoretic mobility of MKP-3–GFP (Fig. 1A). While MKP-3–GFP appears as a single 65-kDa band (Fig. 1A, bottom arrow) in unstimulated cells, its electrophoretic mobility was gradually modified following serum addition (Fig. 1A, upper arrow). After 20 min, the higher-molecular-weight form became the major form of MKP-3–GFP. Interestingly, the intensity of the signal for MKP-3–GFP decreased after 60 min, suggesting that the mobility shift could be associated with a destabilization of the protein.

To rule out the possibility that the shift of MKP-3–GFP depends on the presence of GFP itself, we also tested cell clones expressing tetracycline-inducible MKP-3. Figure 1B shows that serum stimulation modified the apparent molecular weight of native MKP-3. However, MKP-3 is much more unstable than MKP-3–GFP (24), and therefore, the serum-induced shift in electrophoretic mobility was more easily visualized when cells were preincubated with the proteasome inhibitors LLnL (Fig. 1B) or lactacystin (data not shown). This finding suggested the hypothesis that the phosphorylation of MKP-3 could accelerate its degradation by the proteasome. We therefore investigated whether MKP-3 was subjected to ubiquitination. To this end, HeLa cells were cotransfected with the plasmid coding for MKP-3 and with a plasmid coding for His-tagged ubiquitin. After 30 h, cells were lysed, and His-ubiquitin conjugates were purified. Figure 1C shows that polyubiquitinated MKP-3, visible as ladders, could be precipitated from cells transfected with both plasmids. Treating cells with the proteasome inhibitor LLnL for the last 6 h before lysis increased the amount of ubiquitinated MKP-3. This result indicates that the proteasome is a major route for the degradation of MKP-3.

Preincubating the cells with cycloheximide prior to serum

stimulation did not prevent the mobility shift (see below), indicating that this modification was posttranslational. Therefore, we tested whether the mobility shift of MKP-3 was the result of its phosphorylation. Figure 1D shows that the serum-induced electrophoretic mobility of MKP-3 was totally abolished following in vitro dephosphorylation of cell lysates with the CIP. This result clearly indicates that the serum-induced shift in the electrophoretic mobility of MKP-3 is due to its phosphorylation.

Phosphorylation and degradation of MKP-3 depends on the MEK1/2-ERK1/2 pathway. The cell line in which the expression of MKP-3 or MKP-3–GFP can be induced by tetracycline also expresses the ΔRaf1:ER chimera, which allows direct and specific activation of the MEK-ERK pathway by estradiol or 4-OHT (24). Because serum strongly activates the MEK-ERK pathway as well as other signaling pathways, we tested whether exclusive activation of the MEK-ERK module by the ΔRaf1:ER chimera could reproduce the phosphorylation induced by serum. Figure 2A shows that 4-OHT also caused a decrease in MKP-3–GFP mobility, although it started later than with serum, 30 min after the beginning of the stimulation. Phosphorylation of MKP-3 induced by 4-OHT was, however, independent of protein neosynthesis, like serum stimulation (Fig. 2B). The delay in MKP-3 phosphorylation observed with 4-OHT compared to serum, which varies slightly between experiments, may be due to the kinetics of ERK1/2 phosphorylation under the two conditions. While serum triggers a rapid but transient burst of ERK activity, stimulation of the ΔRaf1:ER chimera causes a gradual but long-lasting activation of ERKs (20, 21), as shown in Fig. 2A. Alternatively, this delay may indicate that other signaling pathways cooperate in, and possibly accelerate, MKP-3 phosphorylation by the MEK-ERK pathway.

Note, as we reported previously (24), that the expressed MKP-3–GFP chimera is active in dephosphorylating serum-stimulated ERK2 (Fig. 2A, compare lanes 9 and 10 of the left panel). MKP-3–GFP seems to be even more efficient at later time points (Fig. 2A, left panel; compare lanes 5 and 6 with lanes 9 and 10), even though it is phosphorylated and subjected to degradation. This result is related to the spatiotemporal regulation of phosphorylated ERK (phosphoERK) signaling. At early time points, MKP-3 and its substrate phosphoERK are found in different cellular compartments, with a large part of the phosphoERK signal being in the nucleus, protected from the exclusively cytosolic MKP-3. However, the phosphoERK signal declines much more rapidly in the nucleus than in the cytosol (31, 39). Hence, at later time points, phosphoERK is mainly found in the cytosol, where it can be readily dephosphorylated by MKP-3.

The critical role of the MEK-ERK pathway in serum-induced phosphorylation of MKP-3 was confirmed with U0126, a pharmacological inhibitor of MEKs, which completely blocked the mobility shift of MKP-3–GFP induced by serum (Fig. 2C). In contrast, neither the inhibition of p38 and JNK, two other members of the MAPK family, nor the direct activation of p38 MAPK by anisomycin had any effect on MKP-3 phosphorylation (Fig. 2C).

Although the results obtained with U0126 demonstrate the role of MEKs in the phosphorylation of MKP-3 induced by serum, they do not allow for discrimination between the MEK1/2-ERK1/2 and the MEK5-ERK5 pathways (15), the latter being activated by certain stress and proliferative stimuli, including serum growth factors (14, 16). Because ERK5 is also a substrate for MKP-3 (14), its potential role was to be defined. To this end, we tested whether the specific inhibition of MEK1/2 was sufficient to block the phosphorylation of MKP-3 induced by serum by using PD184352, previously shown to be specific to MEK1/2 at 2 μM while also being able to inhibit MEK5 at 20 μM in HeLa cells (26). Another report showed that even 20 μM PD184352 was not sufficient to block ERK5 activation in CCL39 cells, from which cell lines used in the present study are derived, whereas it efficiently inhibited ERK1/2 at a low dose (36). Figure 2D shows that PD184352 efficiently blocked the phosphorylation of ERK1/2 induced by serum in a dose-dependent manner. In contrast, we confirmed the results reported by Squires et al. (36) that even at a concentration of 20 μM, PD184352 could not block the serum-induced activation of ERK5, visualized as a shift. Interestingly, it seemed that PD184352 even promoted ERK5 activation in serum-stimulated cells, suggesting a negative control of the MEK5-ERK5 pathway by the classical ERK cascade, as previously described (26). U0126 efficiently blocked both ERK5 and ERK1/2 at 10 μM but was less efficient on ERK5 activation when used at 1 μM. Figure 2D also shows that low doses of both U0126 and PD184352 abolish the phosphorylation of MKP-3 induced by serum, suggesting that the MEK5-ERK5 pathway does not play a significant role in the phosphorylation of MKP-3 induced by serum, at least in the cellular model used in this study.

We have shown in Fig. 1 that the phosphorylation of MKP-3 correlates with its degradation by the proteasome. To demonstrate that the two mechanisms are truly connected, we analyzed the effects of the MEK1/2 inhibitor U0126 on MKP-3 stability, using ERK2 levels as a loading control. To avoid any dilution of the signal upwards, which may be confused with a degradation of the molecule, proteins were run on SDS-PAGE (12% acrylamide) for this particular experiment, as shown in Fig. 2E. Therefore, the shift of MKP-3, though visible, is less stressed than in other figures, for which 7.5 or 10% acrylamide gels were used. Corresponding quantification of MKP-3 levels are shown in Fig. 2E. U0126 protected MKP-3 from degradation, especially at late time points. However, this protection was partial, suggesting that other signaling pathways are involved in the destabilization of MKP-3 by serum.

Phosphorylation of endogenous MKP-3. We next investigated whether endogenous, and not only tetracycline-induced, MKP-3 was phosphorylated upon activation of the MEK-ERK module. Parental cells expressed very low levels of endogenous MKP-3, but transcription can be induced by long-term stimulation of the ΔRaf1:ER chimera expressed in these cells (24). Parental cells were thus arrested for 16 h in the presence of [^{33}P]orthophosphate and stimulated with 4-OHT for 4 h to induce both the expression and the phosphorylation of endogenous MKP-3. Cell lysates were then immunoprecipitated for either MKP-3 or an irrelevant protein taken as a negative control. Autoradiography of the Western blot revealed the presence of a phosphoprotein of 45 kDa immunoprecipitated by the anti-MKP-3 antibody in cells treated for 4 h with 4-OHT (Fig. 3A). Immunolabeling with the anti-MKP-3 antibody confirmed that this protein was MKP-3. Addition of the protea-

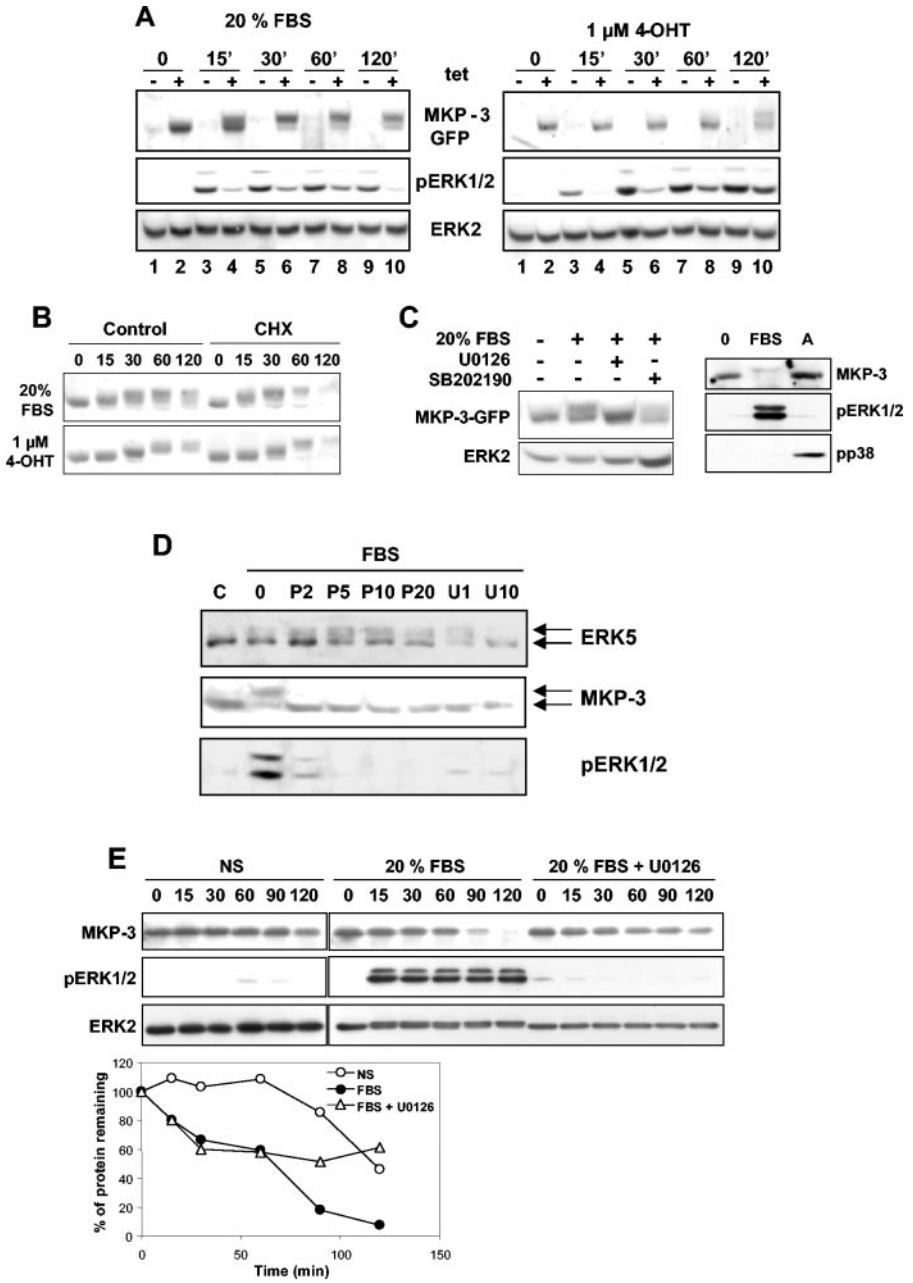

FIG. 2. Phosphorylation of MKP-3 depends on the MEK1/2-ERK1/2 pathway. (A) Stimulation of the ΔRaf1:ER chimera by 4-OHT induced the phosphorylation of MKP-3–GFP. Cells expressing MKP-3–GFP were starved overnight and stimulated for the indicated times with either 20% FBS or 1 μM 4-OHT. The mobility of MKP-3–GFP as well as that of phosphoERK1/ERK2 were analyzed by Western blotting. ERK2 levels were taken as a loading control. (B) Phosphorylation of MKP-3 induced by either serum or 4-OHT is independent of protein synthesis. Cells were treated as described for panel A, but cycloheximide (10 μg/ml) was added or not 30 min prior to serum or 4-OHT stimulation. (C) ERKs but not p38/JNK MAPKs are involved in the phosphorylation of MKP-3. (Left panel) Cells expressing MKP-3–GFP under the control of tetracycline were starved overnight, pretreated with either 10 μM U0126 or 10 μM SB202190 for 30 min, and stimulated with 20% serum for 20 min. Phosphorylation of MKP-3–GFP was analyzed by Western blotting. Levels of ERK2 were taken as a loading control. (Right panel) Cells were starved overnight and treated with either 20% FBS or 1 μg of anisomycin (A)/ml. Phosphorylation of MKP-3–GFP was analyzed by Western blotting. The phosphorylation of ERK1/2 and p38 MAPK are shown as controls for serum and anisomycin stimulation, respectively. (D) ERK5 is not involved in serum-induced phosphorylation of MKP-3. Cells were starved overnight, pretreated with either U0126 (1 or 10 μM) or PD184352 (P; 2 to 20 μM) for 60 min, and stimulated for 30 min with 20% FBS. Cells were lysed and assayed for ERK5, ERK1/2, and MKP-3 phosphorylation. Note the phosphorylation of ERK5, visualized as a shift. (E) Inhibition of MEK-ERK stabilizes MKP-3 in serum-stimulated cells. Cells were starved overnight and stimulated or not with 20% FBS. When indicated, cells were pretreated with 10 μM U0126 for 30 min before FBS stimulation. Cells were lysed, and levels of MKP-3 and pERK1/2 were analyzed by Western blotting. Levels of ERK2 were taken as a loading control.

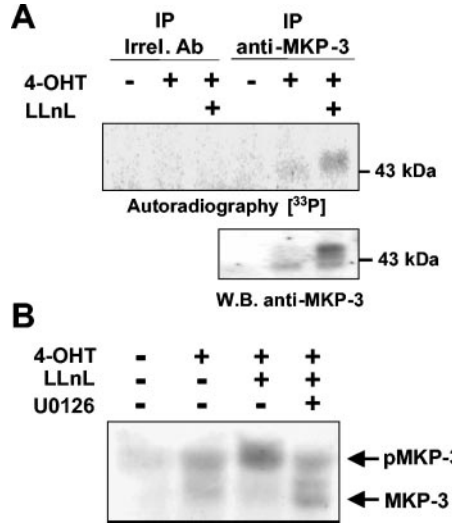

FIG. 3. Activation of the MEK→ERK pathway induced the phosphorylation of endogenous MKP-3. (A) Parental S19 cells, expressing the ΔRaf1:ER, were metabolically labeled with [^{33}P]orthophosphate and stimulated for 4 h with 1 μM 4-OHT in the presence of LLnL. Cells were then lysed, and lysates were immunoprecipitated with either an anti-MKP-3 antibody or an irrelevant antibody. Precipitated proteins were separated on SDS-PAGE, and gels were either exposed for autoradiography or transferred for Western blotting analysis with the anti-MKP-3 antibody. (B) Parental S19 cells were treated for 4 h with 1 μM 4-OHT to activate the ΔRaf1:ER chimera in the presence or in the absence of LLnL. When indicated, U0126 (10 μM) was added during the last hour of 4-OHT treatment.

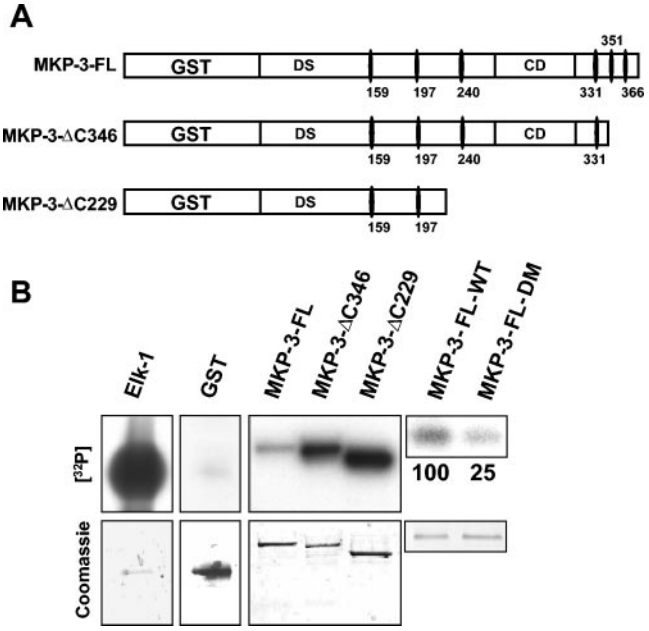

FIG. 4. Recombinant, constitutively activated ERK2 phosphorylates MKP-3 in vitro. (A) Schematic structures of full-length and truncated GST–MKP-3 chimeric proteins. Positions of putative ERK1/2 phosphorylation sites are indicated. DS, docking site; CD, catalytic domain. (B) Phosphorylation of GST–MKP-3 chimeras by ERK2. GST–MKP-3-FL, GST–MKP-3-ΔC346, and GST–MKP-3-ΔC229 were assayed for phosphorylation by ERK2 in vitro. GST–MKP-3-FL-WT (wild type) and GST–MKP-3-FL-DM, mutated on both serine 159 and serine 197, were also compared for the ability to be phosphorylated by ERK2. GST–Elk-1 and GST were taken as positive and negative controls for phosphorylation, respectively. Proteins were then run on SDS-PAGE, and gels were stained with Coomassie blue and exposed for autoradiography. Phosphorylation of GST–MKP-3-FL-WT and GST–MKP-3-FL-DM were quantified and compared by using Coomassie blue staining as a control. When phosphorylation of GST–MKP-3-FL-WT was set as 100%, mutation of both serine 159 and serine 197 (GST–MKP-3-FL-DM) resulted in an 80% decrease in phosphorylation.

some inhibitor LLnL, which stabilized the higher-molecular-weight form of MKP-3, strongly increased the amount of phosphoMKP-3, confirming that the phosphorylated form of MKP-3 is also the most unstable (Fig. 3A). Figure 3B, in which the analysis of MKP-3 in total cell lysates by Western blotting is shown, confirms the stabilizing effect of LLnL on the phosphorylated form of endogenous MKP-3 and shows that pretreating cells with 10 μM U0126 during the last hour of 4-OHT stimulation decreases both the phosphorylation and the degradation of MKP-3.

ERK2 phosphorylates MKP-3 in vitro. The experiments described above, using either 4-OHT or U0126, strongly suggest an involvement for ERK1 and ERK2 in the phosphorylation of MKP-3. The simplest hypothesis is that MKP-3 could be a direct substrate for ERKs. Examination of the primary sequence of MKP-3 revealed the presence of six putative phosphorylation sites for ERKs. GST fusion proteins that comprise full-length or truncated forms of MKP-3, containing all 6, 4, or only 2 putative ERK phosphorylation sites, were produced (schematically depicted in Fig. 4A). Chimeric GST–MKP-3 proteins were incubated with phosphorylated, constitutively active ERK2. GST–Elk-1 was taken as a positive control for phosphorylation by ERK2. ERK2 incorporated ^{32}P in full-length GST–MKP-3 with more efficiency than in GST alone, indicating that MKP-3 is a substrate for ERK2 in vitro. Interestingly, the C-terminal deletion mutant of MKP-3, GST–MKP-3-ΔC346, was a much better substrate for ERK2 (Fig. 4B, left panel). One hypothesis for this result could be that truncation may alter the phosphatase activity of MKP-3, lowering its efficiency towards its substrate, phosphoERK2, in the reaction. We therefore tested the phosphorylation of GST fusion proteins containing either a full-length or a truncated version of a phosphatase-dead mutant of MKP-3, MKP-3-C/S (13). Once again, the truncated GST–MKP-3-C/S-ΔC346 behaved as a better substrate than full-length GST–MKP-3-C/S (data not shown), indicating that the increased phosphorylation of the ΔC346 forms is not due to an alteration of the phosphatase activity of MKP-3 by C-terminal truncation. Alternatively, phosphorylation may be facilitated by conformational changes in the molecule caused by the deletion of the C terminus.

GST–MKP-3-ΔC229, which corresponds to an additional truncation deleting the catalytic domain, was phosphorylated to the same extent as GST–MKP-3-ΔC346. As GST–MKP-3-ΔC229 still contains two potential phosphorylation sites, this result suggested that in vitro phosphorylation of MKP-3 occurs in the N-terminal domain of the protein.

Although the truncated mutants behave as better ERK2 substrates than full-length MKP-3, we did not introduce single amino acid mutations into those truncated proteins for fear that they may have led to artifactual conclusions. Rather, we

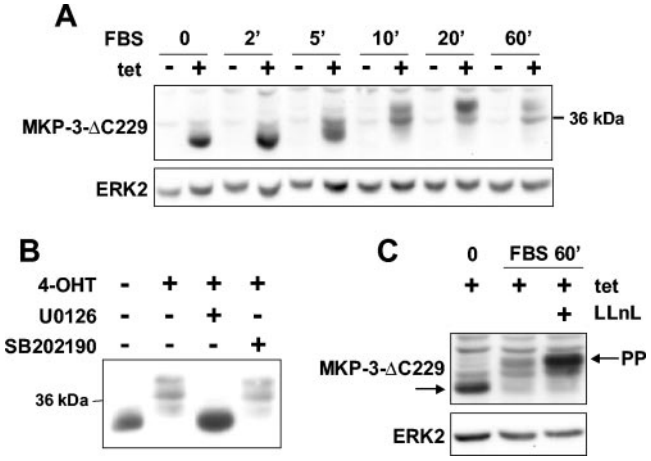

FIG. 5. In vivo phosphorylation of MKP-3 occurs on residues contained in the MKP-3-ΔC229 truncation mutant. (A) Serum induces the phosphorylation of MKP-3-ΔC229. Cells expressing the MKP-3-ΔC229 truncation mutant under the control of tetracycline were starved overnight and stimulated with FBS for the indicated times (in minutes). The shift in mobility was analyzed by Western blotting, and ERK2 levels were taken as a loading control. (B) Phosphorylation of MKP-3-ΔC229 is dependent on the MEK1/2 activity. Cells inducible for MKP-3-ΔC229 expression were starved overnight in the presence of tetracycline, pretreated with either U0126 (10 μM) or SB202190 (10 μM) for 30 min, and stimulated with 1 μM 4-OHT for 2 h. (C) Phosphorylated MKP-3-ΔC229 accumulates in the presence of LLnL. Cells expressing MKP-3-ΔC229 were starved overnight and stimulated or not with serum in the presence or in the absence of the proteasome inhibitor LLnL. ERK2 levels were taken as a loading control.

tested the phosphorylation of a double mutant form of GST–MKP-3-FL, in which both serine 159 and serine 197, contained in the N-terminal region, were replaced by alanine residues. Figure 4B, right panel, shows that wild-type MKP-3 (MKP-3-FL-WT) was more phosphorylated than the double serine mutant (MKP-3-FL-DM). Quantification of the signal revealed a 75% decrease for double mutant phosphorylation compared to wild-type MKP-3 phosphorylation. This result suggests that serines 159 and 197 of MKP-3 are at least targets for ERK2 in vitro.

In vivo phosphorylation of MKP-3 occurs mainly on Ser159 and Ser197. Our next goal was to check the ability of MKP-3 mutants to be phosphorylated in vivo, using the tetracycline-inducible system. Tetracycline-inducible stable cell clones that expressed either the C-terminal truncated forms of MKP-3 (ΔC346 and ΔC229) or the single or double serine mutants of full-length MKP-3 were established. Several stable transfectant clones were isolated for each mutant that provided analogous results.

Serum stimulation induced a shift of MKP-3-ΔC229 truncated proteins (Fig. 5A), confirming the finding that phosphorylation predominantly occurs in the N-terminal domain of MKP-3. Similar results were obtained with the MKP-3-ΔC346 truncation mutant (data not shown). Experiments performed with MKP-3-ΔC229 even revealed two steps in the molecular weight shift, suggesting the existence of two phosphorylation sites. Incubating cell lysates in the presence of CIP confirmed that the shift of MKP-3-ΔC229 was indeed due to its phosphorylation (data not shown). As with full-length MKP-3, this phosphorylation could be induced by stimulation of the ΔRaf1:ER chimera and was blocked by the MEK1/2 inhibitor U0126 but not by the p38 and JNK inhibitor SB202190 (Fig. 5B). Again, addition of LLnL strongly increased the signal of the highest-molecular-weight form (Fig. 5C). Thus, phosphorylation of the MKP-3-ΔC229 truncation mutant shares many similarities with phosphorylation of full-length MKP-3.

Since in vitro experiments indicated that C-terminal deletion could alter phosphorylation stoichiometry (Fig. 4) and may not be truly representative of physiological conditions, we turned to full-length MKP-3 or MKP-3–GFP coding sequences for introducing the serine-to-alanine point mutations. Figure 6A shows that both MKP-3-S159A and MKP-3-S197A gave a mobility shift due to phosphorylation, although it seemed that phosphorylation was more affected in the serine 159 mutant. However, phosphorylation was completely blocked when both serines were mutated (MKP-3-DM). This result clearly establishes that both serine 159 and serine 197 are phosphorylated in response to serum.

Cell clones expressing either wild-type or serine mutants of MKP-3–GFP were also analyzed. The following experiment was performed with cycloheximide-pretreated cells in order to investigate the role of S159 and S197 in the stability of the chimeric phosphatase. Equal amounts of cell lysate protein were compared, and ERK2 levels were taken as a loading control. Again, MKP-3-S197A–GFP shifted in much the same way as wild-type MKP-3–GFP (MKP-3-WT–GFP), and phosphorylation of MKP-3–GFP was much more affected by the serine 159 mutation. Most importantly, phosphorylation of MKP-3-DM–GFP was strongly inhibited (Fig. 6B). The blot shown in Fig. 6B also suggests that MKP-3-DM–GFP was efficiently protected from degradation 90 min after serum addition compared to its wild-type counterpart. Both serines appeared to be involved in this regulation, as the degradation of single mutants was intermediate to that of the wild-type and the double mutant (Fig. 6B).

Serum-induced degradation of the wild-type and double mutant of MKP-3–GFP was also analyzed at later time points for cycloheximide-treated cells and compared to the intrinsic stability of each protein in unstimulated conditions (Fig. 6C). Levels of MKP-3 were quantified by using ERK2 levels as a loading control. The respective stabilities of MKP-3-WT–GFP and MKP-3-DM–GFP were not significantly different in quiescent cells. In contrast, MKP-3-DM–GFP proved to be much more stable than its wild-type counterpart in serum-stimulated cells. Hence, MKP-3-WT–GFP displayed a half-life of 60 min, while that of MKP-3-DM–GFP reached 200 min. Double mutant MKP-3 (uncoupled to GFP) was also more stable than its wild-type counterpart (data not shown).

Together, these results indicate that the phosphorylation of MKP-3 upon activation of the ERK1/2 pathway leads to the rapid degradation of the phosphatase and that both serine 159 and serine 197, which are part of phosphorylation sites for ERKs, are involved in this regulation.

Phosphorylation of MKP-3 does not modify its catalytic activity. Previous works have shown that MKP-3 is catalytically activated by direct binding to purified ERK2, linked to GST or not. Using *p*-NPP hydrolysis as a measure of MKP-3 phosphatase activity, here we show that GST-ERK1 is also able to efficiently activate the phosphatase activity of GST–MKP-3.

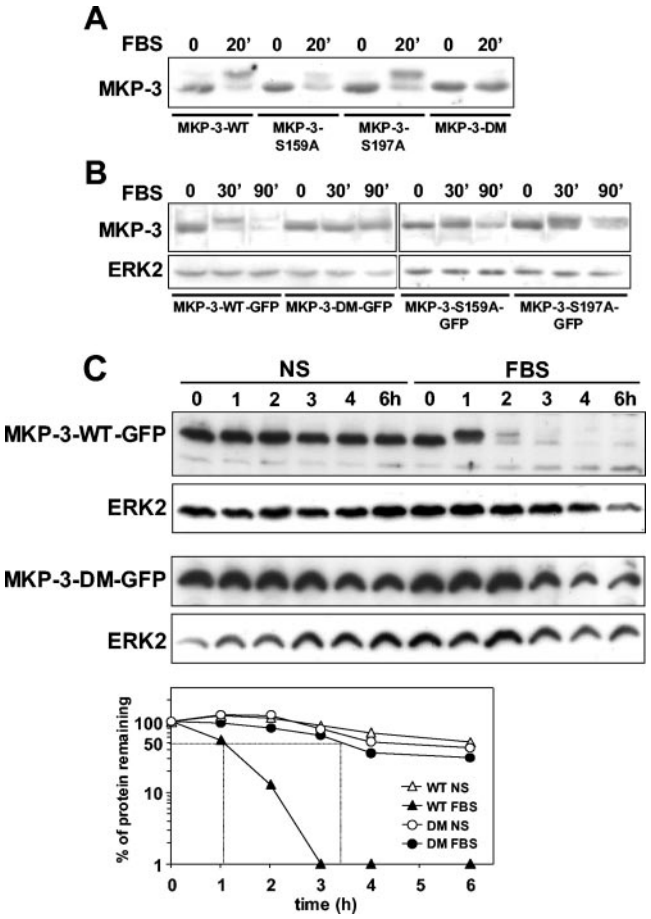

FIG. 6. Role of serine 159 and serine 197 in the phosphorylation and destabilization of MKP-3. (A) Mutation of both serine 159 and serine 197 abolishes MKP-3 phosphorylation. Cell clones expressing either wild-type MKP-3, MKP-3-S159A, MKP-3-S197A, or the double mutant (DM) of MKP-3 were starved overnight and stimulated with serum for 20 min. Proteins were then analyzed by Western blotting. (B) Mutation of both serine 159 and serine 197 abolishes the phosphorylation of MKP-3–GFP but stabilizes it. Tetracycline-inducible cell clones expressing either the wild type or serine mutants of MKP-3–GFP were starved overnight, pretreated with 1 μg of cycloheximide/ml, and stimulated with 20% FBS for 30 or 90 min. The levels of ERK2 were taken as a loading control. (C) Increased stability of MKP-3-DM–GFP. Cells expressing either the wild type or the double mutant MKP-3 were starved overnight, pretreated with 1 μg of cycloheximide/ml, and treated or not treated (NS) with serum for the indicated times. The graph shows the time course of degradation of MKP-3-WT–GFP and MKP-3-DM–GFP under nonstimulated or serum-stimulated conditions. MKP-3 levels were quantified with a Gene Gnome (Syngene Bio Imaging), taking ERK2 levels as a loading control.

Increasing amounts of GST–MKP-3 (5, 10, or 20 μg) were incubated in a *p*-NPP-containing phosphatase reaction buffer, in the presence or in the absence of 10 μg of GST-ERK1. Figure 7A shows that the catalytic activities of the WT and DM forms of GST–MKP-3 are similar. GST-ERK1 (10 μg) increased this activity up to 20-fold when 5 or 10 μg of GST–MKP-3 were used. If a significant basal catalytic activity was observed with 20 μg of GST–MKP-3-WT or GST–MKP-3-DM alone, it was largely increased by adding GST-ERK1 in the reaction (up to sixfold). These data indicate that the mutation of serines 159 and 197 does not, per se, interfere with ERK1 binding on MKP-3.

Next, we analyzed the potential effects of MKP-3 phosphorylation on its catalytic activity. For this purpose, GST–MKP-3-WT and GST–MKP-3-DM were first incubated in kinase buffer in the presence of a recombinant active ERK2 and in the presence (phosphorylated) or absence (unphosphorylated) of ATP. GST–MKP-3 phosphorylation was monitored by ^{33}P incorporation. Proteins were next incubated in phosphatase buffer in the presence of 10 μg of GST-ERK1. Figure 7B shows that phosphorylation of GST–MKP-3 did not modify the course of *p*-NPP hydrolysis.

MKP-3-DM–GFP also proved to be as efficient as MKP-3-WT–GFP in dephosphorylating ERK1/2 in cells (Fig. 7C) (in this experiment, cells were not treated with cycloheximide), indicating again that its inability to be phosphorylated is due to the disruption of phosphorylation sites for ERK1/2 rather than to an impairment of the interaction with ERK1/2.

Finally, Fig. 7D shows that the cytosolic localization of MKP-3–GFP (previously described in reference 24) was not affected by the mutation of serines 159 and 197. Similar results were obtained for native MKP-3 (uncoupled to GFP) and its double mutant (data not shown).

DISCUSSION

Using a tetracycline-inducible system, we have shown that stimulation of the MEK1/2-ERK1/2 pathway by either serum or direct activation of a ΔRaf1:ER chimera resulted in the phosphorylation of the MAPK phosphatase MKP-3, visualized by reduced mobility on SDS-PAGE. This phosphorylation also occurred on endogenous MKP-3 and led to the degradation of MKP-3 by the proteasome machinery. Mutation of serines 159 and 197 in MKP-3 prevented both its phosphorylation and serum-induced degradation in vivo, suggesting that MKP-3 destabilization is a direct consequence of ERK activation. Both serines seemed to be involved in this regulation, as double mutation was most efficient in stabilizing the phosphatase. Finally, we have shown that the phosphorylation of MKP-3 does not affect its catalytic activity.

Serines 159 and 197 are both followed by a proline residue, a hallmark of putative phosphorylation sites for cyclin-dependent kinases and for enzymes of the MAPK family, including ERK1, ERK2, ERK5, p38 MAPK, JNK, and their isoforms. The hypothesis that MKP-3 is a direct substrate for ERK1/2 is strongly supported by four lines of evidence. First, specific activation of the MEK-ERK pathway through activation of the ΔRaf1:ER chimera mimicked the phosphorylation of MKP-3 induced by serum. Second, pharmacological inhibition of MEK1/2 with U0126 completely abolished MKP-3 phosphorylation, while neither the inhibition of JNK/p38 MAPK nor direct activation of p38 by anisomycin had any effect. Inhibition of cyclin-dependent kinases did not affect MKP-3 phosphorylation either (data not shown). Third, a potential role for the MEK5-ERK5 cascade was ruled out on the basis of results obtained with another pharmacological inhibitor, PD184352, more specific to MEK1/2. Fourth, MKP-3 was found to be an in vitro substrate of recombinant active ERK2, and this phosphorylation was strongly reduced when serines 159 and 197 were replaced by alanines. It should also be noted that

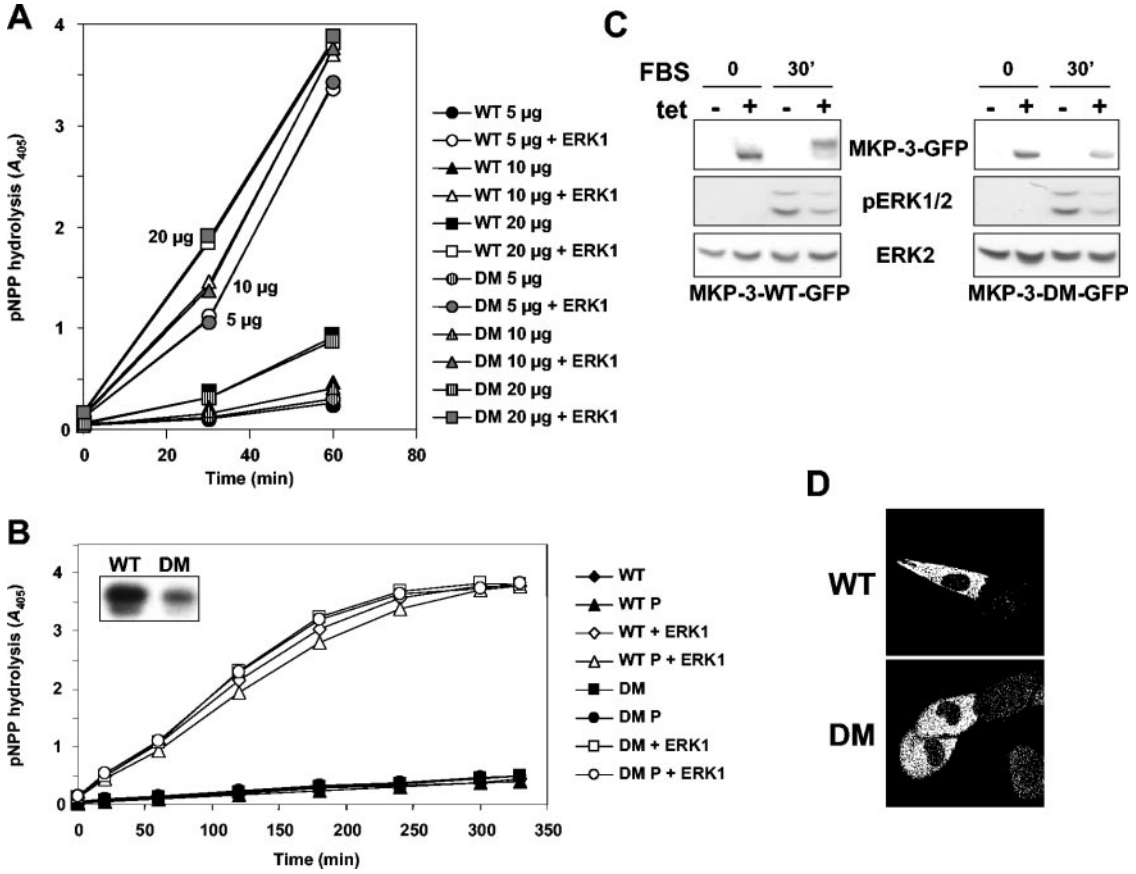

FIG. 7. The phosphorylation of MKP-3 does not modify its phosphatase activity. Phosphatase activity was measured as *p*-NPP hydrolysis at 25°C monitored at an absorbance of 405 nm (A_{405}). GST–MKP-3 and GST-ERK1 were expressed in *Escherichia coli* cells and purified on glutathione-Sepharose. (A) Mutation of serines 159 and 197 does not modify the in vitro phosphatase activity of MKP-3. Increasing amounts of GST–MKP-3-WT or the DM (5, 10, or 20 μg) were incubated in the phosphatase reaction buffer in the absence or in the presence of 10 μg of GST-ERK1 for the indicated times. Note that the reaction rates are similar with GST–MKP-3-WT and the DM. This figure is representative of results from three different experiments. (B) Phosphorylation of MKP-3 does not modify its catalytic activity. GST–MKP-3-WT or the DM were first phosphorylated (indicated by a P) or not by recombinant active ERK2 and incubated in phosphatase reaction buffer with or without 10 μg of GST-ERK1 for the indicated times. Phosphorylation was monitored by ^{32}P incorporation, shown in the upper left corner of the graph. This figure is representative of results from five different experiments. (C) The double mutant of MKP-3–GFP (MKP-3-DM–GFP) efficiently dephosphorylates ERK1/2. Cells expressing either the wild type or the double serine mutant of MKP-3 were starved overnight in the presence of tetracycline and stimulated for the indicated times (in minutes) with 20% serum. Phosphorylation of MKP-3 and ERK1/2 were analyzed by Western blotting using appropriate antibodies. ERK2 levels were taken as a loading control. (D) MKP-3-DM–GFP retains a cytosolic localization. Cells were grown on coverslips and treated overnight with tetracycline to induce either MKP-3-WT–GFP or MKP-3-DM–GFP expression, then fixed, processed for immunofluorescence using the anti-MKP-3 antibody, and observed by confocal microscopy (Leica). Note the cytosolic localization of both MKP-3-WT–GFP and MKP-3-DM–GFP, the background staining in the nucleus also being present in cells that do not express MKP-3–GFP (cells on the right side of the photograph).

p90RSK, a direct substrate for ERKs, is probably not responsible for MKP-3 phosphorylation, as serines 159 and 197 are not included in classical consensus sites for this protein kinase. Together our results suggest that the protein kinases responsible for MKP-3 phosphorylation upon serum stimulation are ERK1 and ERK2.

This essential role of the MEK-ERK pathway in MKP-3 phosphorylation does not exclude, however, the potential participation of other serum-induced signaling pathways, as suggested by the partial protection provided by the MEK inhibitor U0126 to MKP-3 degradation. Such signals might even promote or accelerate the MEK-ERK-dependent phosphorylation of MKP-3, which could explain why the phosphorylation of MKP-3 triggered by the direct activation of the ΔRaf1:ER chimera occurs later than that induced by serum.

The hypothesis that MKP-3 is a substrate for ERKs is further supported by previous reports that MKP-3 is able to form a stable complex with ERKs, notably through the N-terminal domain of the phosphatase (13), although other regions may be involved (42). This interaction is required for efficient and specific inactivation of ERK1/2, as an amino-terminally truncated version of MKP-3 exhibits a nonspecific and much-reduced activity toward all MAPKs (7, 27). Although serines 159 and 197 are situated N-terminally to the MKP-3 catalytic domain, their mutation does not impair the interaction between the phosphatase and ERKs. Indeed, the double mutant of

MKP-3 dephosphorylates ERK1/2 in cells and hydrolyzes *p*-NPP in vitro as efficiently as its wild-type counterpart, a reaction that requires the catalytic activation of MKP-3 through direct binding of ERK (7, 11, 12, 29, 33, 37, 41, 42). Therefore, the inability of the double mutant to be phosphorylated is probably caused by the mutation of phosphorylation consensus sites for ERKs rather than by the disruption of the interaction between MKP-3 and ERKs.

The present report also shows that the phosphorylation of MKP-3 by ERK2 does not modify the catalytic activity of the phosphatase. This result may have been expected, since a kinase-dead mutant of ERK2 is equally effective in activating MKP-3 in vitro (7). However, our results clearly indicate that ERK1/2 exert a novel regulatory role on MKP-3 at the level of its stability. The involvement of the proteasome machinery in MKP-3 degradation was confirmed by both pharmacological inhibition and cotransfection studies with histidine-tagged ubiquitin, which showed that MKP-3 was polyubiquitinated. Numerous studies have implicated ERKs in the regulation of protein stability, either in the destabilization of their substrates or, on the contrary, in their protection against ubiquitination. For example, ERKs were shown to phosphorylate and promote proteasome-dependent degradation of the proapoptotic protein BimEL (22, 23), while phosphorylation by the same protein kinases protects, on the contrary, the antiapoptotic Bcl2 from degradation (2). In the context of cell growth, ERK-mediated phosphorylation facilitates the targeting of inducible cyclic AMP early repressor, an important mediator of cyclic AMP antiproliferative activity, to the proteasomal machinery (40). Interestingly, the regulation of protein stability by ERK phosphorylation takes place even within the enzymatic machinery responsible for the extinction of ERK signaling. This is notably the case for MKP-1 and MKP-2, two other members of the DUSP family, whose phosphorylation by ERK has been previously reported (3). However, it is interesting in the present context that phosphorylation by ERKs has the opposite effect on the fates of MKP-1 and MKP-2, as it protected them from degradation by the proteasome, reinforcing negative feedback on the ERK module.

Surprisingly, a lack of MKP-1 does not impair mouse development or ERK inactivation in fibroblasts (8), suggesting that other phosphatases may compensate for its loss. Compensation may involve MKP-2, which shares with MKP-1 the same nuclear localization, substrate specificity, and ERK-dependent phosphorylation site at the C terminus (6, 18, 38). In sharp contrast, MKP-3 null mutation in *Drosophila* results in embryonic lethality and severe defects in oogenesis (19). Further insights into its developmental role were provided by other recent work performed on chick embryos (10, 17). These striking phenotypes are probably related to the unique features of MKP-3 within the DUSP family, including its cytosolic localization combined with its high specificity toward ERK1 and ERK2. The discovery of novel posttranslational modifications of MKP-3, like the one described in this study, could therefore significantly advance the understanding of its biological roles.

Hence, our findings suggest a model in which the targeting of MKP-3 to the proteasome may account for some aspects of the spatiotemporal regulation of ERK signaling. It is well known that growth factors induce a strong burst of ERK activation and the translocation of active ERK to the nucleus. However, the cytosol remains positive for phosphoERK for a much longer time than the nucleus (31, 39). If MKP-1 and MKP-2 are good candidates for the extinction of the ERK signal in the nucleus, MKP-3 may be crucial for its termination in the cytosol. Because the MKP-3 gene is rapidly induced by growth factors (5; P. Lenormand, personal communication), the only way to maintain sustained ERK activity in the cytosol during G_1 progression would be to decrease MKP-3 activity, with the proteasome providing an efficient solution. At later time points, the balance between active ERK and MKP-3 levels probably shifts in favor of the phosphatase, which eventually leads to the extinction of ERK signaling in the cytosol.

ACKNOWLEDGMENTS

This work was supported by grants from the EEC (QLRT-2000-02278), the Fondation de France, the Association pour la Recherche Contre le Cancer, the Ligue Contre le Cancer, the CNRS, the Ministère de la Recherche, and the University of Nice-Sophia-Antipolis.

We are grateful to Montserrat Camps for her kind advice on the in vitro phosphatase assay and to Anne Doye and Emmanuel Lemichez for their help with ubiquitination experiments. We also thank all members of the laboratory and especially Philippe Lenormand for helpful discussion, Caroline Medioni for her help with confocal microscopy, and Christiane Brahimi-Horn for critical reading of the manuscript.

REFERENCES

1. **Alessi, D. R., N. Gomez, G. Moorhead, T. Lewis, S. M. Keyse, and P. Cohen.** 1995. Inactivation of p42 MAP kinase by protein phosphatase 2A and a protein tyrosine phosphatase, but not CL100, in various cell lines. Curr. Biol. **5:**283–295.
2. **Breitschopf, K., J. Haendeler, P. Malchow, A. M. Zeiher, and S. Dimmeler.** 2000. Posttranslational modification of Bcl-2 facilitates its proteasome-dependent degradation: molecular characterization of the involved signaling pathway. Mol. Cell. Biol. **20:**1886–1896.
3. **Brondello, J. M., J. Pouyssegur, and F. R. McKenzie.** 1999. Reduced MAP kinase phosphatase-1 degradation after p42/p44MAPK-dependent phosphorylation. Science **286:**2514–2517.
4. **Brunet, A., D. Roux, P. Lenormand, S. Dowd, S. Keyse, and J. Pouyssegur.** 1999. Nuclear translocation of p42/p44 mitogen-activated protein kinase is required for growth factor-induced gene expression and cell cycle entry. EMBO J. **18:**664–674.
5. **Camps, M., C. Chabert, M. Muda, U. Boschert, C. Gillieron, and S. Arkinstall.** 1998. Induction of the mitogen-activated protein kinase phosphatase MKP3 by nerve growth factor in differentiating PC12. FEBS Lett. **425:**271–276.
6. **Camps, M., A. Nichols, and S. Arkinstall.** 2000. Dual specificity phosphatases: a gene family for control of MAP kinase function. FASEB J. **14:**6–16.
7. **Camps, M., A. Nichols, C. Gillieron, B. Antonsson, M. Muda, C. Chabert, U. Boschert, and S. Arkinstall.** 1998. Catalytic activation of the phosphatase MKP-3 by ERK2 mitogen-activated protein kinase. Science **280:**1262–1265.
8. **Dorfman, K., D. Carrasco, M. Gruda, C. Ryan, S. A. Lira, and R. Bravo.** 1996. Disruption of the erp/mkp-1 gene does not affect mouse development: normal MAP kinase activity in ERP/MKP-1-deficient fibroblasts. Oncogene **13:**925–931.
9. **Doye, A., A. Mettouchi, G. Bossis, R. Clement, C. Buisson-Touati, G. Flatau, L. Gagnoux, M. Piechaczyk, P. Boquet, and E. Lemichez.** 2002. CNF1 exploits the ubiquitin-proteasome machinery to restrict Rho GTPase activation for bacterial host cell invasion. Cell **111:**553–564.
10. **Eblaghie, M. C., J. S. Lunn, R. J. Dickinson, A. E. Munsterberg, J. J. Sanz-Ezquerro, E. R. Farrell, J. Mathers, S. M. Keyse, K. Storey, and C. Tickle.** 2003. Negative feedback regulation of FGF signaling levels by Pyst1/MKP3 in chick embryos. Curr. Biol. **13:**1009–1018.
11. **Farooq, A., G. Chaturvedi, S. Mujtaba, O. Plotnikova, L. Zeng, C. Dhalluin, R. Ashton, and M. M. Zhou.** 2001. Solution structure of ERK2 binding domain of MAPK phosphatase MKP-3: structural insights into MKP-3 activation by ERK2. Mol. Cell **7:**387–399.
12. **Fjeld, C. C., A. E. Rice, Y. Kim, K. R. Gee, and J. M. Denu.** 2000. Mechanistic basis for catalytic activation of mitogen-activated protein kinase phosphatase 3 by extracellular signal-regulated kinase. J. Biol. Chem. **275:**6749–6757.
13. **Groom, L. A., A. A. Sneddon, D. R. Alessi, S. Dowd, and S. M. Keyse.** 1996. Differential regulation of the MAP, SAP and RK/p38 kinases by Pyst1, a novel cytosolic dual-specificity phosphatase. EMBO J. **15:**3621–3632.
14. **Kamakura, S., T. Moriguchi, and E. Nishida.** 1999. Activation of the protein kinase ERK5/BMK1 by receptor tyrosine kinases. Identification and char-

acterization of a signaling pathway to the nucleus. J. Biol. Chem. **274:**26563–26571.
15. **Karihaloo, A., D. A. O'Rourke, C. Nickel, K. Spokes, and L. G. Cantley.** 2001. Differential MAPK pathways utilized for HGF- and EGF-dependent renal epithelial morphogenesis. J. Biol. Chem. **276:**9166–9173.
16. **Kato, Y., V. V. Kravchenko, R. I. Tapping, J. Han, R. J. Ulevitch, and J. D. Lee.** 1997. BMK1/ERK5 regulates serum-induced early gene expression through transcription factor MEF2C. EMBO J. **16:**7054–7066.
17. **Kawakami, Y., J. Rodriguez-Leon, C. M. Koth, D. Buscher, T. Itoh, A. Raya, J. K. Ng, C. R. Esteban, S. Takahashi, D. Henrique, M. F. Schwarz, H. Asahara, and J. C. Izpisua Belmonte.** 2003. MKP3 mediates the cellular response to FGF8 signalling in the vertebrate limb. Nat. Cell Biol. **5:**513–519.
18. **Keyse, S. M.** 2000. Protein phosphatases and the regulation of mitogen-activated protein kinase signalling. Curr. Opin. Cell Biol. **12:**186–192.
19. **Kim, M., G.-H. Cha, S. Kim, J. H. Lee, J. Park, H. Koh, K.-Y. Choi, and J. Chung.** 2004. MKP-3 has essential roles as a negative regulator of the Ras/mitogen-activated protein kinase pathway during *Drosophila* development. Mol. Cell. Biol. **24:**573–583.
20. **Le Gall, M., J. C. Chambard, J. P. Breittmayer, D. Grall, J. Pouyssegur, and E. Van Obberghen-Schilling.** 2000. The p42/p44 MAP kinase pathway prevents apoptosis induced by anchorage and serum removal. Mol. Biol. Cell **11:**1103–1112.
21. **Lenormand, P., M. McMahon, and J. Pouyssegur.** 1996. Oncogenic Raf-1 activates p70 S6 kinase via a mitogen-activated protein kinase-independent pathway. J. Biol. Chem. **271:**15762–15768.
22. **Ley, R., K. Balmanno, K. Hadfield, C. Weston, and S. J. Cook.** 2003. Activation of the ERK1/2 signaling pathway promotes phosphorylation and proteasome-dependent degradation of the BH3-only protein, Bim. J. Biol. Chem. **278:**18811–18816.
23. **Luciano, F., A. Jacquel, P. Colosetti, M. Herrant, S. Cagnol, G. Pages, and P. Auberger.** 2003. Phosphorylation of Bim-EL by Erk1/2 on serine 69 promotes its degradation via the proteasome pathway and regulates its proapoptotic function. Oncogene **22:**6785–6793.
24. **Marchetti, S., C. Gimond, D. Roux, E. Gothie, J. Pouyssegur, and G. Pages.** 2004. Inducible expression of a MAP kinase phosphatase-3-GFP chimera specifically blunts fibroblast growth and ras-dependent tumor formation in nude mice. J. Cell. Physiol. **199:**441–450.
25. **Milanini-Mongiat, J., J. Pouyssegur, and G. Pages.** 2002. Identification of two Sp1 phosphorylation sites for p42/p44 mitogen-activated protein kinases: their implication in vascular endothelial growth factor gene transcription. J. Biol. Chem. **277:**20631–20639.
26. **Mody, N., J. Leitch, C. Armstrong, J. Dixon, and P. Cohen.** 2001. Effects of MAP kinase cascade inhibitors on the MKK5/ERK5 pathway. FEBS Lett. **502:**21–24.
27. **Muda, M., A. Theodosiou, C. Gillieron, A. Smith, C. Chabert, M. Camps, U. Boschert, N. Rodrigues, K. Davies, A. Ashworth, and S. Arkinstall.** 1998. The mitogen-activated protein kinase phosphatase-3 N-terminal noncatalytic region is responsible for tight substrate binding and enzymatic specificity. J. Biol. Chem. **273:**9323–9329.
28. **Muda, M., A. Theodosiou, N. Rodrigues, U. Boschert, M. Camps, C. Gillieron, K. Davies, A. Ashworth, and S. Arkinstall.** 1996. The dual specificity phosphatases M3/6 and MKP-3 are highly selective for inactivation of distinct mitogen-activated protein kinases. J. Biol. Chem. **271:**27205–27208.
29. **Nichols, A., M. Camps, C. Gillieron, C. Chabert, A. Brunet, J. Wilsbacher, M. Cobb, J. Pouyssegur, J. P. Shaw, and S. Arkinstall.** 2000. Substrate recognition domains within extracellular signal-regulated kinase mediate binding and catalytic activation of mitogen-activated protein kinase phosphatase-3. J. Biol. Chem. **275:**24613–24621.
30. **Pearson, G., F. Robinson, T. Beers Gibson, B. E. Xu, M. Karandikar, K. Berman, and M. H. Cobb.** 2001. Mitogen-activated protein (MAP) kinase pathways: regulation and physiological functions. Endocr. Rev. **22:**153–183.
31. **Pouyssegur, J., V. Volmat, and P. Lenormand.** 2002. Fidelity and spatiotemporal control in MAP kinase (ERKs) signalling. Biochem. Pharmacol. **64:**755–763.
32. **Reffas, S., and W. Schlegel.** 2000. Compartment-specific regulation of extracellular signal-regulated kinase (ERK) and c-Jun N-terminal kinase (JNK) mitogen-activated protein kinases (MAPKs) by ERK-dependent and non-ERK-dependent inductions of MAPK phosphatase (MKP)-3 and MKP-1 in differentiating P19 cells. Biochem. J. **352:**701–708.
33. **Rigas, J. D., R. H. Hoff, A. E. Rice, A. C. Hengge, and J. M. Denu.** 2001. Transition state analysis and requirement of Asp-262 general acid/base catalyst for full activation of dual-specificity phosphatase MKP3 by extracellular regulated kinase. Biochemistry **40:**4398–4406.
34. **Smith, D. B., and K. S. Johnson.** 1988. Single-step purification of polypeptides expressed in Escherichia coli as fusions with glutathione S-transferase. Gene **67:**31–40.
35. **Sohaskey, M. L., and J. E. Ferrell, Jr.** 2002. Activation of p42 mitogen-activated protein kinase (MAPK), but not c-Jun NH(2)-terminal kinase, induces phosphorylation and stabilization of MAPK phosphatase XCL100 in Xenopus oocytes. Mol. Biol. Cell **13:**454–468.
36. **Squires, M. S., P. M. Nixon, and S. J. Cook.** 2002. Cell-cycle arrest by PD184352 requires inhibition of extracellular signal-regulated kinases (ERK) 1/2 but not ERK5/BMK1. Biochem. J. **366:**673–680.
37. **Stewart, A. E., S. Dowd, S. M. Keyse, and N. Q. McDonald.** 1999. Crystal structure of the MAPK phosphatase Pyst1 catalytic domain and implications for regulated activation. Nat. Struct. Biol. **6:**174–181.
38. **Theodosiou, A., and A. Ashworth.** 2002. MAP kinase phosphatases. Genome Biol. **3:**reviews3009.1–3009.10. [Online.]
39. **Volmat, V., M. Camps, S. Arkinstall, J. Pouyssegur, and P. Lenormand.** 2001. The nucleus, a site for signal termination by sequestration and inactivation of p42/p44 MAP kinases. J. Cell Sci. **114:**3433–3443.
40. **Yehia, G., F. Schlotter, R. Razavi, A. Alessandrini, and C. A. Molina.** 2001. Mitogen-activated protein kinase phosphorylates and targets inducible cAMP early repressor to ubiquitin-mediated destruction. J. Biol. Chem. **276:**35272–35279.
41. **Zhao, Y., and Z. Y. Zhang.** 2001. The mechanism of dephosphorylation of extracellular signal-regulated kinase 2 by mitogen-activated protein kinase phosphatase 3. J. Biol. Chem. **276:**32382–32391.
42. **Zhou, B., L. Wu, K. Shen, J. Zhang, D. S. Lawrence, and Z. Y. Zhang.** 2001. Multiple regions of MAP kinase phosphatase 3 are involved in its recognition and activation by ERK2. J. Biol. Chem. **276:**6506–6515.